Triplet State Dynamics in Peridinin-Chlorophyll-*a*-Protein: A New Pathway of Photoprotection in LHCs?

Maxime T. A. Alexandre,* Daniel C. Lührs,* Ivo H. M. van Stokkum,* Roger Hiller,† Marie-Louise Groot,* John T. M. Kennis,* and Rienk van Grondelle*

*Department of Biophysics and Physics of Complex Systems, Division of Physics and Astronomy, Faculty of Sciences, Vrije Universiteit, De Boelelaan 1081, 1081 HV Amsterdam, The Netherlands; and †Department of Biology, Macquarie University, Sydney, New South Wales 2109, Australia

ABSTRACT This work investigates the interaction of carotenoid and chlorophyll triplet states in the peridinin-chlorophyll-*a*-protein (PCP) of *Amphidinium carterae* using step-scan Fourier transform infrared spectroscopy. We identify two carotenoid triplet state lifetimes of ~13 and ~42 μs in the spectral region between 1800 and 1100 cm^{-1} after excitation of the 'blue' and 'red' peridinin (Per) conformers and the Q_y of chlorophyll-*a* (Chl-*a*). The fast and slow decaying triplets exhibit different spectral signatures in the carbonyl region. The fast component generated at all excitation wavelengths is from a major conformer with a lactone stretching mode bleach at 1745 cm^{-1}. One (1720 cm^{-1}) and two (1720 cm^{-1} and 1741 cm^{-1}) different Per conformers are observed for the slow component upon 670- and 530–480-nm excitation, respectively. The above result implies that ^{3}Per triplets are formed via two different pathways, corroborating and complementing visible triplet-singlet (T-S) spectra (Kleima et al., Biochemistry (2000), *39*, 5184). Surprisingly, all difference spectra show that Per and Chl-*a* modes are simultaneously present during the ^{3}Per decay, implying significant involvement of ^{3}Chl-*a* in the ^{3}Per state. We suggest that this Per-Chl-*a* interaction via a delocalized triplet state lowers the ^{3}Per energy and thus provides a general, photoprotection mechanism for light-harvesting antenna complexes.

INTRODUCTION

Photosynthetic organisms use antenna pigment-protein complexes for harvesting light energy and for transferring the excitation energy to the reaction center (RC), where it is converted into an electrochemical potential leading ultimately to NADH and ATP synthesis (1). To do so, dinoflagellates use the water-soluble peridinin-chlorophyll-*a*-protein (PCP), a major light-harvesting (LH) pigment protein in conjunction with a light-harvesting complex (LHC) of the conventional three-transmembrane type (2). PCP is the LH protein with the highest carotenoid/chlorophyll ratio: four peridinins (Pers) per chlorophyll-*a* (Chl-*a*). This ratio, as well as the small number of chromophores per protein, makes PCP a perfect model system for studying the photoprotection mechanism by carotenoids.

The photochemical properties of carotenoids are determined to a great extent by the length of their π-electron conjugation and the nature of the functional groups attached on the conjugated chain (3,4). Per has an unusual C_{37} carbon skeleton rather than the typical C_{40} system present in most carotenoids (Fig. 1). The unique structure of Per is constituted of an allene moiety and a lactone ring in conjugation with the π-electron system of the carotenoid backbone, an epoxy group with a secondary alcohol group on one β-ring, and an ester group located on the opposite β-ring with a tertiary alcohol group. The structural differences between Per and other carotenoids are most likely related to its unusual function in PCP; in contrast to most photosynthetic LHCs, Per, and not Chl-*a*, is the main light-absorbing pigment in PCP.

Per absorbs light in the 470–550-nm region and is extremely efficient at harvesting light in photosynthetic antenna pigment-protein complexes (5–8). In PCP, the efficiency for Per-Chl-*a* excitation energy transfer (EET) is ~90% (5,9,10). Such high efficiency is achieved by tight packing, at van der Waals radii, of the pigments, minimizing the distances between donor (Per) and acceptor (Chl-*a*) molecules. The 2.0-Å crystal structure of PCP from the dinoflagellate *Amphidinium carterae* reveals a trimeric arrangement (2). Monomeric PCP contains eight Pers and two Chl-*a* molecules, which are densely packed and arranged in two essentially similar units each consisting of four Pers clustered around one Chl-*a* molecule.

Per in PCP not only has an exceptional LH function, but it is also very efficient in photoprotecting protein and chromophore from degradation by singlet oxygen, as 100% of Chl-*a* triplet is quenched (9,11). Singlet oxygen can be formed by the quenching of chlorophyll triplet states:

$$^3\text{Chl-}a^* + {}^3O_2 \rightarrow \text{Chl-}a + {}^1O_2^* \text{ (singlet oxygen formation)}.$$

To prevent this reaction, carotenoids (Car) with their low-lying triplet states quench long-lived chlorophyll triplets (12–17) and scavenge singlet oxygen (18):

$$^3\text{Chl-}a^* + \text{Car} \rightarrow \text{Chl-}a + {}^3\text{Car}^* \text{ (chlorophyll triplet quenching)}$$

Submitted February 15, 2007, and accepted for publication April 17, 2007.

M. T. A. Alexandre and D. C. Lührs contributed equally to this work.

Address reprint requests to R. van Grondelle, E-mail: R.van.Grondelle@few.vu.nl.

Editor: Dagmar Ringe.

0006-3495/07/09/2118/11 $2.00

doi: 10.1529/biophysj.107.106674

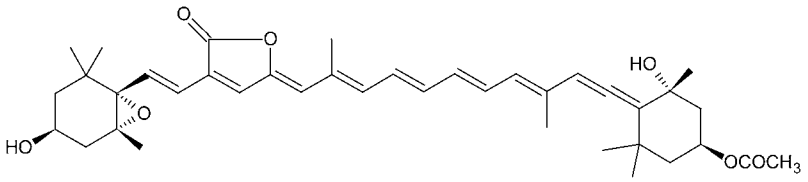

FIGURE 1 Molecular structure of Per.

$^1O_2^* + Car \rightarrow {}^3O_2 + {}^3Car$ (singlet oxygen scavenging).

The lowest triplet energy level of carotenoids with nine or more conjugated double bonds is assumed to be lower than that of singlet oxygen (19,20), which lies at 7882 cm^{-1} (21,22). The carotenoid triplet does not react with ground state oxygen, thus preventing the generation of singlet oxygen, and is for the same reason able to scavenge singlet oxygen. Per has eight double bonds in the backbone, conjugated to a ninth double bond of the carbonyl group in the lactone ring. Considering the molecular features that make Per an efficient light harvester—the strong electronegative oxygen atoms of the lactone ring (Fig. 1) and the structural perturbation by the protein environment (2)—the triplet state energy of Per conformers might be just at an energy threshold for quenching singlet oxygen. Typically, unquenched chlorophyll triplets display lifetimes in the orders of a few milliseconds, long enough to lead to singlet oxygen formation and a subsequent damage of the LH apparatus. Under such conditions, both the L and M subunits of the carotenoidless RC from *Rhodobacter sphaeroides* were uniformly photodamaged (23).

In PCP, the triplet states of Chl-*a* are formed via intersystem crossing (ISC) from Chl-*a* singlet states. The latter are formed after direct Chl-*a* excitation or after EET, which follows direct excitation of Per (9,10,24). The Per triplet states are populated by triplet excitation energy transfer (TEET), which is governed by an electron-exchange interaction (Dexter mechanism) (22,25). Kleima et al. (11) found a Per triplet lifetime of 10 μs at room temperature (RT) and 13 and 40 μs for 77 K and four Per conformers to be involved in the triplet state formation, consistent with the 10 μs Per lifetime found by Bautista et al. (9) at RT and the two lifetimes of 13 and 58 μs reported by Carbonera et al. (26) within a temperature range from 2 to 200 K and assigned to the anisotropy of the triplet sublevel dynamics. The PCP visible triplet-singlet (T-S) spectra (11,27) exhibit a Q_y Chl-*a* differential signal assigned to Chl-*a*-carotenoid interaction and is similar to carotenoid T-S spectra found in bacterial and higher plant antennae (28–30). This interaction signal shows concerted dynamics with the carotenoid triplet (11,28) and has been discussed in terms of a Stark effect, but its exact nature remains unclear. To investigate the nature of the Per triplet state in more detail, we have measured the ^{3}Per dynamics in the *A. carterae*, Per-Chl-*a*-protein (A-PCP) using time-resolved step-scan Fourier transform infrared spectroscopy (FTIR) in the region 1100–1800 cm^{-1} after either direct Per or Chl-*a* excitation. With time-resolved step-scan FTIR, we monitor excitation-induced variations in vibrational modes. We observe that ^{3}Chl-*a* coexists with ^{3}Per, as they have the same dynamics, and suggest that delocalization of the triplet over the Per and the Chl-*a* is responsible for the conspicuous Q_y bleach in visible T-S spectra. In addition we report that the triplet dynamics are excitation wavelength dependent, implying that ^{3}Per triplets in PCP are formed via two different pathways.

MATERIALS AND METHODS

Sample preparation

Samples of PCP of *A. carterae* were prepared as previously described (2). Droplets of 20 μL of PCP solution, containing 10 mg/mL PCP, 25 mM Tris Cl (pH 7.5) buffer, 3 mM NaN_3, 2 mM KCl, were concentrated under nitrogen flow on a CaF_2 window. The resulting paste (3–5 μL) was spread between two tightly fixed CaF_2 windows.

The high concentration of ~60 mg/mL implies that 99% of PCP was in the trimeric form. The optical density (0.3 for 670 nm) and homogeneity of the sample were checked before and after each experiment by recording ultraviolet/visible (250–700 nm) and midinfrared (1800–1100 cm^{-1}) steady-state spectra to ensure reproducible experimental conditions.

Time-resolved step-scan FTIR absorption measurements

The time-resolved interferograms were recorded at RT using a step-scan FTIR spectrometer (IFS 66s Bruker, Billerica, MA) placed on an air-bearing table (Kinetic Systems, Boston, MA). A globar infrared (IR) light source and a fast preamplified photovoltaic MCT detector (20 MHz, KV 100, Kolmar Technologies) were used. The IR light impinging on the sample was sent through 1850 cm^{-1} and 4000 cm^{-1} low-pass filters, which blocked the laser light before the interferometer and the detector. The detector signal was recorded with an external digitizer (PAD 82a; Spectrum Labs, Rancho Dominguez, CA; 100 MHz, 8-bit analog to digital (A/D) converter) for 1-μs time resolution and with the internal digitizer (200 kHz, 16-bit A/D converter) for 5-μs time resolution. A 20 Hz, neodymium-doped yttrium aluminum garnet laser (5 ns, 100 mJ at 355 nm, Continuum, Santa Clara, CA) was used to pump an optical parametric oscillator (Panther, Continuum), producing tunable visible light from 400–700 nm, with a pulse duration of 5–7 ns. This light was attenuated to 2 mJ/cm^2 (for all excitation wavelengths), weakly focused to a spot of 4 mm in diameter and overlapped with the IR probe beam, which was slightly smaller. A Stanford Research Systems (Sunnyvale, CA) digital delay generator (DCR 35) was used to vary the time delay between the pump laser pulse and the trigger of the detection electronics.

Data acquisition and analysis

Each three-dimensional IR interferogram has a time resolution of 1 or 5 μs and 660 points for a required resolution of 8 cm^{-1} in a spectral window from 1800 to 1100 cm^{-1}. Every data set is an average of 20 single-sided time-resolved interferograms of which each point is a time slice that is the average of nine coadditions. The time-resolved interferograms have been further Fourier transformed into time-resolved IR difference spectra (OPUS software,

Bruker Optics). For the interpretation of the data we applied a parallel kinetic model and fitted the dynamics of every point of a spectral data set simultaneously with global analysis (31,32). This analysis leads to decay-associated difference spectra (DADS) with associated lifetimes, whose errors have been estimated to be <10%.

Experimental errors and reproducibility

Three lifetimes were needed to sufficiently fit the data. Besides two very intense DADS, a third component of very low intensity (<10%) has been fitted with a lifetime of ~500 μs. However, due to the limited stability of the mirror in the Michelson Interferometer, an artificial millisecond vibration can show up as experimental lifetime error along the time axis, and consequently we exclude the third DADS from our discussion.

Due to the acquisition and FT of interferograms, every point and its dynamics in the spectral data set are a result of several interferogram points and their dynamics. Spectra were reproduced reliably under different laser intensity (10–0.2 mJ/cm^2) conditions and experimental settings, such as time and frequency resolution (1 and 5 μs, 8 and 16 cm^{-1}). At higher laser excitation intensities, the spectral and dynamical information were the same, but the sample would bleach quickly (after some minutes). At lower intensities (<0.5 mJ), the signal/noise ratio was too small, thus we used typically a laser pulse energy of 2 mJ/cm^2. To investigate the excitation wavelength dependence, we carefully set the pump power to 2 mJ/cm^2 for all excitation wavelengths and performed the measurements the same day on the same sample, refreshing the pumped spot twice for each excitation.

Under the above experimental conditions the number of absorbed photons is of the same order of magnitude as the number of Pers contained in the excited volume of the sample, thus with our 5–7-ns pulse the probability for uncontrolled multiphoton processes (33) is rather small. No longer-lived Chl-*a* triplets have been detected, excluding the possibility of free or unquenched Chl-*a*.

RESULTS

Time-resolved step-scan FTIR spectra of PCP triplet states

In this article we use microsecond time-resolved FTIR spectroscopy to measure triplet formation in PCP by monitoring excitation-induced variations in the vibrational modes of the PCP chromophores. In the following paragraphs, we present the estimated lifetimes, the DADS, and the vibrational mode assignment of three sets of time-resolved IR data resulting from excitation of Chl-*a* at 670 nm (Q_y) and Per at 480 nm (maximum of Per absorption) and 530 nm (*red edge* of Per absorption). Excitation at 550 nm gave essentially the same result as at 530 nm (data not shown).

Data analysis/lifetimes

Time-resolved mid-IR spectra were collected and globally analyzed at frequencies between 1100 and 1800 cm^{-1}, and the resulting DADS are shown in Fig. 2. To describe the time-resolved data, we used a parallel model, which required three components: two fast lifetimes, of the order of tens of microseconds and a longer one that we do not consider further (see experimental error section). No components were found in the order of the instrument response of ~5 μs. This was corroborated by measurements with a time resolution of 1 μs yielding the same dynamics (data not shown).

We find the triplet state dynamics of PCP at RT to be described by lifetimes of 13 and 42 μs, which are typical of carotenoid triplets. Previous experiments on PCP in the visible spectral region reported one Per triplet lifetime of 10 μs at RT (9,11) and two lifetimes of 13 and 40 μs at 77 K (11) and 13 and 58 μs up to 200 K (26), respectively. Typical carotenoid triplet lifetimes of light-harvesting complex II (LHCII), peripheral purple bacteria light-harvesting complex (LH2), and PCP are compared in Table 1. Our observation of two triplet lifetimes at RT could be related to our strictly anaerobic experimental conditions. In Fig. 2 the positive DADS signals originate from excited state absorption (ESA) of the triplet states and negative DADS signals from the bleach of the ground state.

Spectral analysis

In our spectral analysis, we distinguish four regions of interest: the carbonyl region (1800–1630 cm^{-1}); the C=C stretch region, characteristic of the polyene backbone of carotenoids and chlorophylls giving rise to bands between 1610 and 1525 cm^{-1}; the CH-deformations and possible lactone ring modes in the region of 1450–1380 cm^{-1}; and the fingerprint region below 1380 cm^{-1} with, e.g., CH-out-of-plane, C-C, and C-O stretches and their combinations (37).

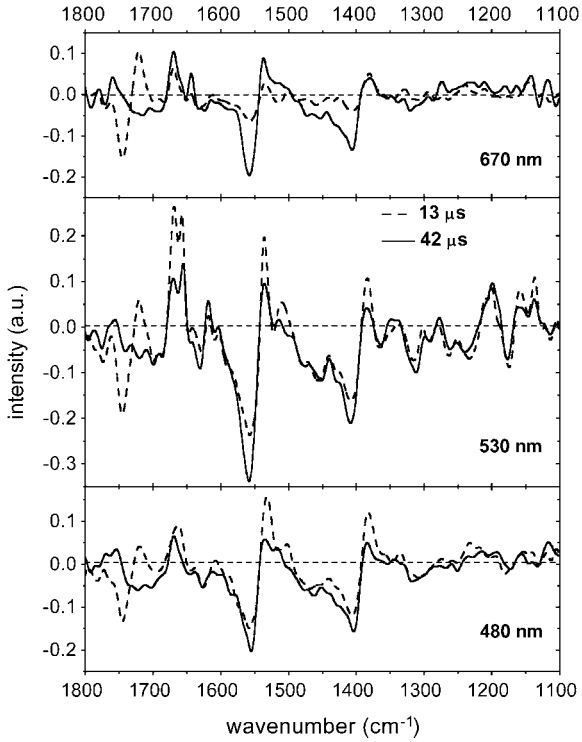

FIGURE 2 DADS of PCP obtained using a parallel model after 670-, 530-, and 480-nm excitation (from *top* to *bottom*). DADS1 (*dashed line*) and DADS2 (*solid line*) are associated with 13- and 42-μs lifetimes, respectively.

TABLE 1 Triplet state lifetimes of carotenoids in several LH complexes at varying excitation wavelengths and temperatures

LH Complex	Lifetimes (μs)	Excitation wavelength	Temperature	Carotenoid
PCP (9,11)	10	590 nm	RT	Peridinin
PCP (11)	13 and 40	590 nm	77 K	Peridinin
PCP (26)	13 and 58	400–600 nm	<200 K	Peridinin
PCP this work	13 and 42	670 nm	RT	Peridinin
		530 nm	RT	
		480 nm	RT	
LH2 (61)	9.5 and 43		4 K	Neurosporene
	3.3 (oxygenic)		RT	
LHCII (28,62)	9 (anaerobic)	462 nm	RT (28,62)	Several (Lutein, Neo-/Violaxanthin)
	2 and 4 (oxygenic)	480 nm	RT (28,62)	
	8 and 40	590 nm	4 K (28)	

C=C stretching and C-H deformation modes

As we can see in Fig. 2, the two DADS show many spectral similarities. The weak bands at 1623/1633 cm^{-1} (bleach) and strong bands at ~1555/1530 cm^{-1} (bleach/ESA) are Per C=C stretching modes. Typically, carotenoid C=C stretching modes are ~1520 cm^{-1}—e.g., spheroidene, β-carotene (34,35)—and downshifted by 20 cm^{-1} to ~1500 cm^{-1} in the T_1 state (34). In Per we observe slightly higher frequencies, indicating a decrease in bond order, as observed normally for peripheral C=C stretches (36). Moreover, the broad band extending from ~1480 cm^{-1} to lower frequencies (bleach) due to CH-deformation modes is characteristic of carotenoids (37). The reported modes of Chl-*a* in PCP (11) at 1610, 1553, and 1526 cm^{-1} might also contribute to these bands to a minor extent. Additional recognizable modes are at ~1450 cm^{-1} the methylene C-H deformation and the methyl asymmetric bending modes, as well as the symmetric methyl bending mode of the Per backbone peaks at 1408/1380 cm^{-1} (bleach/ESA) (37).

Carbonyl region: molecular probes

The carbonyl region contains contributions from Per and Chl-*a* since both have carbonyl groups in conjugation with their electronic system. These carbonyl modes are very sensitive to electronic changes and can be used as molecular probes for the individual chromophores. The carbonyl modes that can be expected in this region are the lactone mode of Per and the 10a-ester and 9-keto modes of Chl-*a* (Fig. 1).

Fig. 3 shows the second derivative of the steady-state FTIR absorption spectrum of the PCP carbonyl region together with the raw data obtained at t_0 by step-scan FTIR for 530- and 670-nm excitation. The FTIR data show carbonyl stretching modes at 1770, 1745, 1725, 1710, 1695, and 1681 cm^{-1} that are all involved in the triplet dynamics as the corresponding bleaches are observed in the raw time-resolved data. The strong amide I band, representing absorption of the protein backbone carbonyl stretch, is located at 1650 cm^{-1} and off scale in Fig. 3. After global analysis, the DADS in the carbonyl region show five major frequencies in the ground state bleach (best resolved with 530-nm excitation): 1745 cm^{-1} (DADS1), 1741, 1720 cm^{-1} (DADS2), 1699, and 1686 cm^{-1} (both DADS) as seen Fig. 4. The slight mismatch observed between the negative bands in the second derivative IR absorption spectrum relative to the time-resolved spectra bleaches is due to the positive absorption that accompanies a band shift.

Carbonyl modes of Chl-*a*

The bands at ~1699, 1686 cm^{-1} (bleach), shown in Fig. 4, match the 1697 and 1681 cm^{-1} ones reported from fluorescence line narrowing (FLN) spectra at 4 K (11). Since no crystallographic evidence has been found for H-bonded Chl-*a* 9-keto in 1PPR (PCP Protein Data Bank code), we assign the 1699-cm^{-1} band to a Chl-*a* in a relatively apolar environment. The ESA of the two bands has shifted down to 1670 and 1657 cm^{-1}, respectively. Such a downshift is typical for the 9-keto vibration of Chl-*a* in T-S FTIR spectra and can be perfectly overlapped with the T-S FTIR spectrum of Chl-*a* in tetrahydrofuran (THF) (38). Chl-*a* triplets are known to exhibit a downshift in the ESA, whereas Chl-*a* cations are upshifted (38–40). A hypothetical charge transfer state leading to Per(+)/Chl-*a*(−) would be expected to downshift the

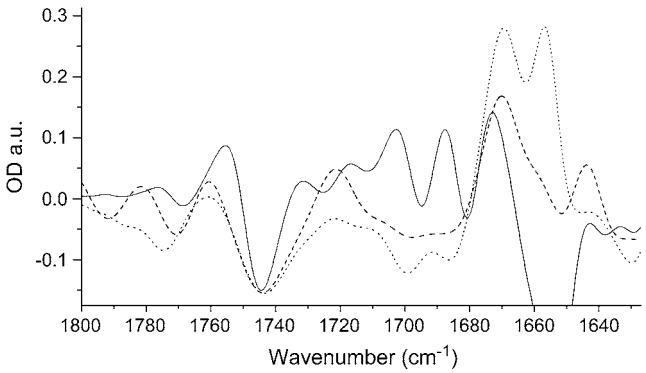

FIGURE 3 PCP carbonyl region of the raw time-resolved data at t_0 obtained after excitation at 670 (*dashed line*) and 530 nm (*dotted line*) compared to the second derivative of PCP FTIR absorption spectrum (*solid line*).

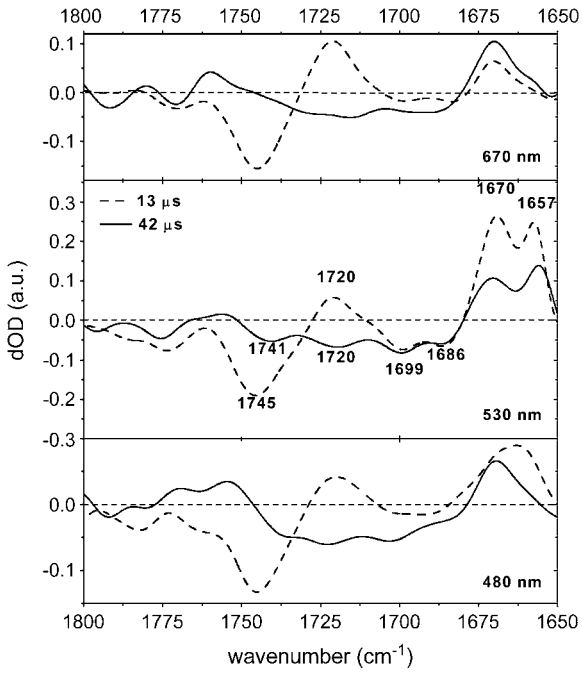

FIGURE 4 Comparison of the carbonyl modes of the PCP DADS at 670-nm, 530-nm, and 480-nm excitation.

9-keto vibration of Chl-*a* anion by ~55–92 cm^{-1} as observed for bacteriopheophytin/bacteriopheophytin$^-$ in THF (41), pheophytin/pheophytin$^-$ in photosytem II (PSII) (42), and bacteriochlorophyll-*a* (BChl-*a*)/BChl-*a*$^-$ (43). In our data the 9-keto vibration of Chl-*a* downshifts by 30 cm^{-1} and strongly suggests that only Chl-*a* triplets exist on typical triplet carotenoid lifetimes and we can exclude the presence of Chl-*a* cations and anions.

ESA of the Chl-*a* 9-keto carbonyl modes is dependent on the excitation wavelength as the envelop centered at 1670 cm^{-1} under 670-nm excitation evolves to a splitting at 1670 cm^{-1} and 1657 $cm^{-1}$for 530-nm excitation (Fig. 4). This suggest that direct Chl-*a* excitation favors the localization of the Chl-*a*/Per triplet on the high-frequency keto carbonyl Chl-*a*, whereas direct red Per excitation populates both Chl-*a* equally. From the 9-keto-mode amplitudes at 1699, 1686 cm^{-1}, we conclude that both Chl-*a* molecules of the quasisymmetric PCP monomer are involved in the triplet state dynamics at RT, however to a different extent depending on the excitation wavelength.

The 9-keto mode is the strongest mode in T-S Chl-*a* FTIR difference spectra, about three times more intense than the 10a-ester mode (38,39), so we assign the other strong carbonyl modes to the lactone vibration of Per.

Carbonyl modes of Per

The remaining three ground state bleach modes—again best resolved after 530-nm excitation—at 1745 cm^{-1} (DADS1), 1741 (DADS2), and 1720 cm^{-1} (DADS2) represent the lactone carbonyl modes of three distinguishable Per conformers; however, the 1741 cm^{-1} (DADS 2) conformer is absent under 670-nm excitation (Fig. 4). The Per ester group, which could be a candidate for these frequencies, is located at one of the cyclo-hexane end groups and isolated from the conjugated backbone (Fig. 1). For this reason, we do not expect contributions of the ester group after electronic excitation. The carbonyl stretch of a five-membered lactone has a typical frequency of 1765 ± 5 cm^{-1} (44), which can downshift by 20 cm^{-1} in conjugation with a π-system, as in Per, and even farther in a polar environment or with hydrogen bonding of the carbonyl to the protein pocket. Moreover, the 25-cm^{-1} downshift of the ESA corresponding to the 1745/1720 cm^{-1} bands would be large compared to 5 cm^{-1} for ester groups (as reported, e.g., for chlorophyll) (39). The observed ground state bleach modes are in agreement with Per resonant (530 nm) Raman data for PCP (E. Papagiannakis and B. Robert, unpublished data), which display only two broad bands at 1745 and 1720 cm^{-1} in the carbonyl region. In addition, the resonant Raman spectrum of Per in methanol shows only one broad carbonyl frequency, peaking around 1740 cm^{-1}.

Assignment of possible protein modes

The highest modes, above 1760 cm^{-1} (1790/1780 and 1770/1760 cm^{-1} DADS2, 670-nm excitation, Fig. 4), for both bleach and ESA bands are rather high in energy to originate from Per lactone, Chl-*a* 10a-ester, or Per ester vibrations; and the downshift of ~10 cm^{-1} is rather small compared to the shift of 25 cm^{-1} observed for Per lactone (1745/1720 cm^{-1} DADS1, 670-nm excitation, Fig. 4). Thus, it is more likely that these modes represent conformational changes of acidic residues as Asp or Glu upon triplet formation, but we cannot exclude a contribution from the Per ester carbonyl.

The spectral assignments summarized in Table 2 lead to the following conclusions:

- All observed modes in the second derivative FTIR spectrum (Fig. 3) are involved in the triplet decay dynamics with bands at 1745, 1741, 1725, and 1710 cm^{-1} and bands at 1695 and 1681 cm^{-1} assigned to various Pers and Chl-*a* conformers, respectively, experiencing different protein environment.
- The 1710-cm^{-1} band clearly observed in the second derivative IR absorption spectrum contributes to a lesser extent to the differential signal; the 1770-cm^{-1} band is likely assignable to acidic side chains of amino acids or ester stretch of Per.
- Differential signals of Per and Chl-*a* are characteristic for their respective triplet states, which disappear with typical carotenoid triplet decay time constants. This implies that in PCP, whereas the triplet is on the Per, the triplet wave function is delocalized over the Chl-*a*, and both triplet signals decay with typical carotenoid triplet lifetimes.

TABLE 2 Spectral assignment of the principal stretching modes

Second derivative PCP spectrum	T-S infrared spectra and DADS (Bleach/ESA)	Vibrational assignment
1770	1770/1760	Asp or Glu side chain or Per ester
1745	1745/1720	Per lactone
nd	1741/nd	Per lactone
1725	1720/nd	Per lactone
1710	nd	Per lactone
1695	1699/1670	Chl-*a* 9-keto
1681	1686/1657	Chl-*a* 9-keto
1628	1630/1619	Per C=C (mainly) and Chl-*a* C=C
1550	1555/1530	Per C=C (mainly) and Chl-*a* C=C

In addition, both Per and Chl-*a* infrared differential signals show an excitation wavelength dependence. The low-frequency keto carbonyl Chl-*a* is more populated and the 1741-cm^{-1} Per conformer appears in DADS2 upon direct red Per excitation (530 and/or 550 nm) in comparison to direct Chl-*a* excitation (670 nm). As seen in Fig. 5 the 1720 cm^{-1} dynamics shows a strong wavelength dependence, suggesting increased population of this Per conformer upon direct Per excitation. These spectral changes are accompanied by an overall increase of signal amplitude observed from 670 to 480 and to 530 nm in Fig. 4. This signal increase is better observed in the raw data before global analysis, as seen in Fig. 6.

DISCUSSION

For the spectral assignments, the carbonyl region is most important, as Per and Chl-*a* possess conjugated carbonyl groups which are sensitive to the protein environment and the electronic state of the pigment. In other words, the carbonyl modes are the molecular probes for the pigments: the 9-keto mode of the Chl-*a* and the carbonyl group of the lactone ring of Per. The keto modes are generally expected at lower energies ($\leq$1700 cm^{-1}) compared to lactone modes (>1700 cm^{-1}), which makes them easily distinguishable.

Chl-*a* modes: coexistence of Chl-*a* and carotenoid triplets

Best resolved are the vibrational modes in the DADS after excitation at 530 nm. In the region below 1700 cm^{-1} the two strong bleach vibrations at 1699 and 1686 cm^{-1} are assigned to Chl-*a* ground state modes on the basis of FLN data (11), resonant (413 nm) Raman data (E. Papagiannakis and B. Robert, unpublished data), and differential FTIR spectroscopy (38). As the observed lifetimes reflect typical carotenoid triplet lifetimes, it is somewhat surprising to observe Chl-*a* modes involved in the DADS. However, a bleach of the Chl-*a* Q_y band at 670 nm with a microsecond lifetime has also been observed in visible (VIS) T-S spectra of PCP (9,11) and LHCII (45). The interpretation was that the Chl-*a* senses the carotenoid triplet and is electronically perturbed. Van der Vos et al. (29) proposed a mechanism in which Chl spectral changes are induced by a change in the electrostatic interaction between the Chl singlet state and a nearby carotenoid in the triplet state. At a short distance such an electronic perturbation can be strong on, e.g., the Chl Q_y, and this could lead to a bleach of the Q_y through band shift or changes in dipole strength. Although a definite excited state species originating from Chl-*a* could not be observed in the visible T-S spectra (10,24), the DADS (Fig. 4) presented here show that the two Chl-*a* ground state modes experience a downshift to 1670 cm^{-1} and 1657 cm^{-1}, respectively. This downshift of ~30 cm^{-1} in the keto mode is typical for an excited triplet

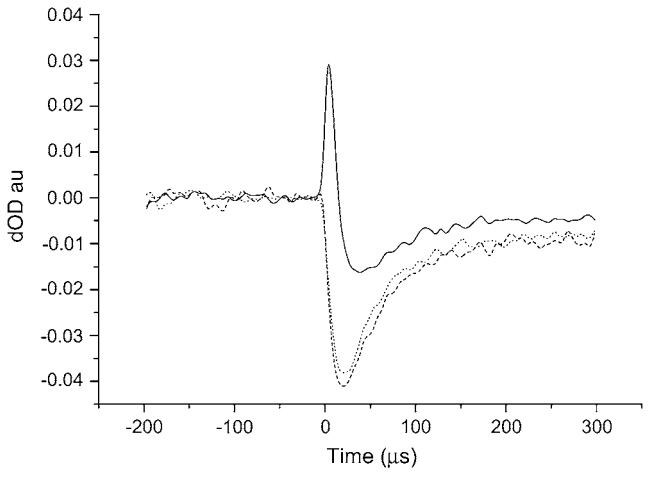

FIGURE 5 PCP time traces for absorbance at 1720 cm^{-1} with 670-nm (*solid line*), 530-nm (*dashed line*), and 480-nm (*dotted line*) excitations.

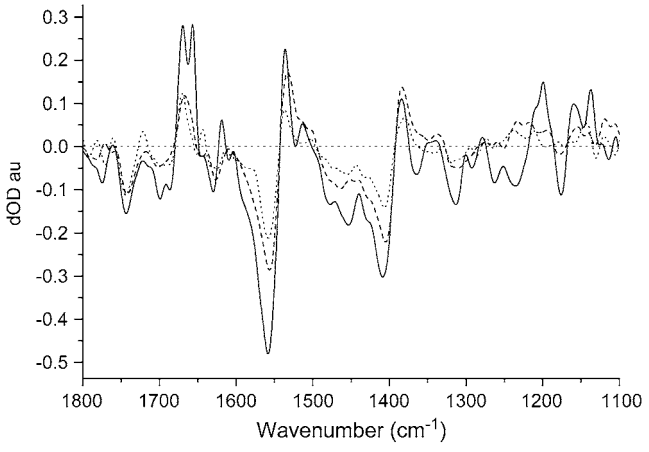

FIGURE 6 Differential absorbance signals of PCP obtained by step-scan FTIR. Raw data are t_0 time slices with 5-μs time resolution for 670-nm (*dotted line*), 480-nm (*dashed line*), and 530-nm (*solid line*) excitation; intensity 2 mJ/cm^2 at all wavelengths.

state (38). Thus, we can assign the Chl-*a* transient species most definitely to Chl-*a* triplet states and can exclude electrostatic interaction or the presence of radical anions or cations (which would exhibit larger down- or upshifted ESA, respectively) (39). Similar amplitudes are observed for the 1745/1720 cm^{-1} bleach/ESA of the Per lactone and the 1699/1670 cm^{-1} bleach/ESA of the Chl-*a* 9 keto, which suggests that a significant fraction of Chl-*a* is in the triplet state, as observed in the T-S spectra of PCP (9,11) and LHCII (45). For the latter it was calculated that the presence of a triplet state on a carotenoid bleaches ~75% of the absorption equivalent of one Chl-*a*. Thus, our interpretation that the Chl-*a* in PCP has a triplet character during the time that Per triplets are present is in agreement with previous nanosecond flash photolysis experiments in the visible T-S spectra (11).

Quenching models for chlorophyll triplet states

The concerted dynamics of Chl-*a* triplets and Per triplets in all our DADS is quite unexpected since all Chl-*a* triplet excitation energy is thought to be finally quenched by Per (5,9,11,46) or carotenoids in general, due to their low-lying triplet states. The classical triplet transfer pathway describes the quenching of chlorophyll triplet states by energetically lower lying carotenoid states. For PCP the following equation describes the mechanism:

$$\text{a.}\ ^3\text{Chl-}a + \text{Per} \rightarrow \text{Chl-}a + ^3\text{Per}.$$

However, this does not explain the experimentally observed coexistence of Per and Chl-*a* triplets at Per lifetimes. To explain the Chl-*a* dynamics on carotenoid lifetimes, two scenarios can be proposed: an equilibrium between Chl-*a* and Per triplet states or a delocalized triplet state in which the triplet is shared by Per and Chl-*a*.

$$\text{b.}\ ^3\text{Chl-}a + \text{Per} \leftrightarrow \text{Chl-}a + ^3\text{Per (equilibrium)}$$

$$\text{c.}\ ^3\text{Chl-}a + \text{Per} \rightarrow ^3[\text{Chl-}a + \text{Per}]\ \text{(delocalized triplet)}.$$

Equilibrium model

One explanation for the concerted chlorophyll triplet dynamics would be a dynamic thermal equilibrium between the Per and Chl-*a* triplet states where the triplet state is deactivated via the fastest pathway, the Per pathway, which might explain the typical carotenoid triplet lifetime. Triplet migration has been reported between Pers in PCP (26), and the thermal equilibration of chlorophyll triplets in PSII-RC (Chl1/P680) has been observed (40). Recent phosphorescence spectroscopy on LH2 antenna complexes (47) has determined the difference of BChl-*a* and carotenoid triplet energy to be only ~500–700 cm^{-1} (BChl T_1 energy 7590 cm^{-1} vs. ~7000 cm^{-1} for carotenoids) and shows coexistence of both BChl and carotenoid triplet in an almost equal amount in the stationary state. The authors interpreted the coexistence of T_1 BChl and T_1 Car as a thermal equilibrium which, however, recombines into a Q_y singlet excited state via triplet-triplet annihilation in ~2 ns. These are equilibria between almost energetically equivalent triplet states, and we observe coexistence of Per and Chl-*a* triplet states in the microsecond timescale. An equilibrium between ^{3}Chl-*a* and ^{3}Per would have to overcome a energy difference of ~2000 cm^{-1}, as the lowest triplet state is estimated to be ~10,000 cm^{-1} for chlorophylls (48) and ~8000 cm^{-1} for ^{3}Per based on a Per S1 of 16,100–16,500 cm^{-1}, where the lowest carotenoid triplet state is estimated to lie at half of the corresponding S_1 energy level (3).

In the context of a thermal equilibrium, we would expect lowering the temperature to favor triplet localization on the carotenoid. The Q_y bleach in the visible T-S spectra has comparable amplitudes at RTs of 77, 40, and 4 K in LHCII and at an RT of 77 K in PCP, which makes the thermal equilibrium rather unlikely.

Delocalized triplet model

Another possibility is that Per and Chl-*a* share the triplet. Microwave-induced absorption (MIA) spectra of bacterial LH show the presence of a Q_y bleach whose intensity is related to the efficiency of TEET in the different complexes (30). Such a delocalization of the carotenoid triplet wave function over an adjacent (B)Chl has been discussed by Angerhofer et al. (30) for bacterial LHC. However the authors concluded that the observed Q_y response upon ^{3}Car formation was probably due to electrostatic perturbation of the (B)Chl upon carotenoid triplet population. Delocalization of the carotenoid triplet state over an adjacent Chl-*a* molecule leading to the mixing of Chl triplet character in the carotenoid triplet state provides a straightforward explanation for the shape of the signal in the visible T-S spectra: bleaching of the Q_y band and a broad featureless absorption increase in this region, as is expected for a Chl-*a* triplet T-S spectrum. Efficient TEET is governed by a Dexter-type exchange interaction. Such a short-range exchange mechanism requires the overlap of donor and acceptor wave functions and thus obeys an exponential law on intermolecular distance. The Dexter mechanism is nearly 100% efficient at a distance of ~3.5 Å. Because the TEET yield in PCP is ~100%, the overlap must be significant, which is consistent with the PCP structure where the protein scaffold encloses a Chl-*a*-Per cluster with the pigments at 3.9–4.5 Å. This is also consistent with the observation of Carbonera et al. (26), who have shown the occurrence of intracluster ^{3}Per migration demonstrating significant highest occupied molecular orbital/lowest unoccupied molecular orbital overlap between the Pers.

Interestingly Angerhofer et al. (30) have shown that in bacterial LH complexes the intensity of the BChl-*a* Q_y bleach in the MIA spectra is directly correlated with the rate of TEET but the Car-BChl interaction is not related to the polyene length ($n = 11,13$). Thus it appears that delocalization of the

triplet wave function between Chl or BChl and carotenoid occurs when the overlap of the ground state and excited state wave functions is predominant over the relative energies of the molecules involved in TEET. This triplet delocalization effect appears to be tightly related to the triplet-triplet coupling strength. A recent calculation on TEET (49) showed that the electronic coupling mainly arises from the region of close contact between the donor and acceptor frontier orbitals and is strongly dependent on the intermolecular configuration. Triplet-triplet coupling strength is optimal and decays less steeply with increasing separation, when acceptor and donor orbitals are fully stacked. Thus, directly stacked π-π overlap between Per and Chl-*a* in PCP should be mainly responsible for the Per triplet wave function delocalization over the neighboring Chl-*a*. The PCP crystal structure exhibits each Chl-*a* surrounded by two stacked (Per 612/622 and 614/624) and two side by side Pers (Per 611/621 and 613/623), of which Per 612/622 has its allene moiety stacked with Chl-*a* at ~4 Å. Thus, Chl-*a* coupling to Per 612/622 together with 614/624 is the more likely candidate for the observed concerted triplet dynamics.

The observation of chlorophyll triplets during the lifetime of the carotenoid triplet identifies the observed 670 nm bleaches in visible T-S spectra of PCP as originating from shared Per-Chl-*a* triplets. Moreover, a similar shared triplet has recently been observed in LHCII and FCP (M. T. A. Alexandre, I. H. M. van Stokkum, J. T. M. Kennis, and R. van Grondelle, manuscript in preparation), corroborating the observation on PCP and pointing toward a general phenomenon and thus possibly a new understanding of the photoprotection mechanism. In this respect, it is important to note that the Chl or (B)Chl Q_y bleach upon carotenoid triplet decay is observed in all LH systems, including artificial ones such as carotenophthalocyanine dyads and triads (50,51).

Per modes

The other specific modes that are active after electronic excitation are the Per lactone modes above 1700 cm^{-1}. Four different modes could be observed—1745, 1741, 1720, and 1710 cm^{-1}—showing that PCP provides different environments for each Per conformer with respect to its backbone and lactone groups. The assignment is corroborated by the Raman frequencies of 1720 and 1745 cm^{-1} in resonance upon 530-nm excitation (E. Papagiannakis and B. Robert, unpublished data). The observation of four lactone modes is in agreement with Kleima et al. (11), who concluded that four different triplet state conformers contributed to their VIS T-S spectra at 77 K.

Origin of DADS1

For all excitation wavelengths the DADS1 show similar intensities of the spectral bands in the carbonyl region with a strong band shift at 1745/1720 cm^{-1}, which represents a first Per conformer. However, an amplitude decrease of the 1720 cm^{-1} ESA is noticeable for 480- and 530-nm excitation, which could be related to participation of an additional conformer after direct Per excitation. This is also suggested by the time trace at 1720 cm^{-1} shown in Fig. 5, where the ESA is visible upon 670-nm excitation, whereas it is compensated by apparent bleach upon 530- and 480-nm excitation. Furthermore, we observe an increase in amplitude of the Chl-*a* band shift (negative at 1699–1686 cm^{-1}, positive at 1670 cm^{-1}–1657 cm^{-1}), which might be associated with the presence of the additive 1720 cm^{-1} Per conformer. Those two conformers, 1745 and 1720 cm^{-1}, represent spectrally the shorter lifetime of 13 μs, with the 1745 cm^{-1} mode corresponding to the highest frequency lactone carbonyl Pers. Below 1600 cm^{-1} in DADS1, all modes are more intense at 530- and 480-nm excitation compared to 670-nm excitation, which is consistent with populations of two and one conformers at such excitation, respectively. The stronger modes' band shifts in the fingerprint region below 1300 cm^{-1} at 530-nm excitation suggest a more distorted, twisted Per triplet conformation.

Origin of DADS2

The intensity and spectral features of the carbonyl region in DADS2 also depend on the initial excitation wavelength. The wavelength dependence is characterized by the appearance of a lactone mode at 1741 cm^{-1} on 530-nm excitation, which is absent on 670-nm excitation together with an increased population of the conformers with carbonyl modes at 1720 cm^{-1} upon 530-nm excitation. The latter changes are more pronounced upon 530-nm excitation and are observed together with an increased ESA of the low-frequency keto Chl-*a* at 1657 cm^{-1}.

The overall amplitude increase observed upon direct Per excitation (Fig. 6) is attributable to both DADS1 and DADS 2 and is associated with the additional participation of 1741 and 1720 cm^{-1} Per conformers compared to direct Chl-*a* excitation.

Thus, it appears that the triplet localization among the Per conformers and the Chl-*a* can be tuned by the initial excitation wavelength. This is surprising as it does not agree with the classical understanding of triplet quenching in LHCs, according to which all excitation energy is expected to be initially collected on the Chl-*a*, no matter whether it was Per or Chl-*a* that was excited (10,24). Such wavelength dependency indicates that the triplet pathway is conformer sensitive and mainly the red Pers (excited at 530 and/or 550 nm, see Results section) change the triplet pathway as well as the localization of the triplet among the two PCP clusters. This suggests that this red Per acts as a switch which triggers an additional excited state pathway and/or a different fate of the excited state among the complex. Perhaps this additional excitation pathway photoprotects the PCP by deactivating Per singlet excited state into harmless Per triplet states. It has

been shown that these red Pers have some specific properties. First, the largest Stark signal is observed for the red Per conformers in PCP at 530–550 nm, which suggests a charge-transfer (ICT) state character (52,53). Second, Salverda (54) proposed a strong interaction between Chl-*a* and red Pers (Per 614/624) to explain the zero-rise time bleach band at 540 nm in the ultrafast transient absorption spectra after Chl-*a* excitation. Salverda suggested a structural rearrangement of Per 614/624 on Chl-*a* excitation as a possible mechanism. Thus a specific interaction between Chl-*a* and this red Per exists. This is consistent with the nonconservative CD signal of the Q_y of Chl-*a* in PCP (11,55), which is explained by an excitonic interaction of Chl-*a* and Per.

The ICT state character of the red Pers and their special interaction with Chl-*a* might be involved in the mechanism that opens an additional triplet deactivation pathway. Several explanations are likely for the formation of different Per triplet states dependent on the excitation wavelength. A first possibility is that the ICT-forming conformers might undergo a structural change by coupling to Chl-*a* and change the triplet equilibrium among and between the Per-Chl-*a* clusters. However, that would imply that on the nanosecond timescale the system is still in a kind of hot vibrational conformational state where it ''remembers'' the red Per excitation, which seems to be unlikely.

Nonetheless, because it appears that exciting the red Pers at 530 and/or 550 nm leads to a significant increase of the 1740 and 1720 cm^{-1} triplet, the more realistic conclusion would be that the 530–550-nm red Pers have their own triplet state generation pathway. Thus, we favor two possibilities. First, these ICT-prone conformers, which exhibit a stark signal comparable to that of the heterodimer special pair of the bacterial RC, could undergo charge separation and lead to triplet generation by radical pair charge recombination as shown in PSII-RC for Chl+ and Phe− (40). The second one could be that the red Pers have a larger ability to undergo the singlet fission mechanism (56). The special mechanism of ultrafast ^{3}Car formation (intramolecular singlet fission), as identified in carotenoids bound in bacterial LHCs (56,57), was not observed in PCP by ultrafast spectroscopy (10,24). However, even if femtosecond experiments did not give any indication of such ultrafast triplet formation, we can wonder if under our excitation conditions permanent conformational changes induced by direct Per excitation could lead to activation of the singlet fission pathway, as this mechanism has been shown to be dependent on the carotenoid distortion (58). Indeed, the light minus dark FTIR spectrum of PCP excited at 530 nm shows subtle (few milliOD) conformational changes assignable to the high-frequency carbonyl Per conformer (1745 cm^{-1}), whereas no changes have been observed upon 670-nm excitation (data not shown). A double-photon process that leads to direct Per triplet and/or radical formation would be another possibility; Per cation radicals have been generated when the S_2 state was repumped with 800-nm light (59). As shown by Billsten et al. (60), excitation of zeaxanthin with a strong nanosecond pulse can lead to triplet and radical formation. Even if the probability is low under our experimental conditions, such a double photon process would explain the overall increased signal (DADS1 and DADS2) and the appearance of the 1741 cm^{-1} conformer together with the 1720 cm^{-1} bleach and 1657 cm^{-1} ESA increase at 530-nm excitation. Thus, the exact mechanism of this excitation wavelength dependency observed by direct red Per excitation remains unclear; however, opening an additional triplet deactivation pathway could have physiological implications as a photoprotective process.

CONCLUSIONS

In this study we distinguish the triplet state forming Per conformers in PCP by their lifetimes and spectral features and find two independent triplet transients at RT. DADS1 represents the typical pathway of carotenoid photoprotection with predominantly 1745 cm^{-1} conformer contributing, whereas the other conformers (predominantly 1741 and 1720 cm^{-1}) show wavelength-dependent triplet formation via a different mechanism than the classical TEET, likely involving the ICT state coupling to Chl-*a* or the singlet fission mechanism.

Furthermore, all DADS show the involvement of both Chl-*a* and Per conformers in the triplet state dynamics at all excitation wavelengths, from which we conclude that the Per triplet wave function extends over the Chl-*a* system. This likely stabilizes Per triplet states well below the oxygen singlet state energy, which lie respectively at ~8000 and 7882 cm^{-1}, providing PCP with the property to quench the singlet oxygen state. Hence, our data show that the two Chl-*a* of the PCP monomer are active in the photoprotection processes undergoing concerted dynamics with the Pers forming a delocalized triplet.

We thank Dr. Emmanouil Papagiannakis for fruitful discussions and for sharing the unpublished resonant Raman data on PCP and Dr. Jacques Breton for fruitful discussions.

M.T.A.A. is supported by the Earth and Life Sciences Council of the Netherlands Organization for Scientific Research (NWO-ALW) in the context of the Molecule to Cell program. J.T.M.K. was supported by NWO-ALW through a VIDI grant.

REFERENCES

1. van Grondelle, R., J. P. Dekker, T. Gillbro, and V. Sundström. 1994. Energy-transfer and trapping in photosynthesis. *Biochim. Biophys. Acta.* 1187:1–65.
2. Hofmann, E., P. M. Wrench, F. P. Sharples, R. G. Hiller, W. Welte, and K. Diederichs. 1996. Structural basis of light harvesting by carotenoids: peridinin-chlorophyll-protein from Amphidinium carterae. *Science.* 272:1788–1791.
3. Christensen, R. L. 1999. The electronic states of carotenoids. *In* The Photochemistry of Carotenoids. H. A. Frank, A. J. Young, M. Braun, and R. J. Cogdell, editors. Kluwer, Dordrecht, The Netherlands. 137–159.

4. Krinsky, N. I. 1971. Function. *In* Carotenoids. O. Isler, G. Guttman, and U. Solms, editors. Birkhäuser, Basel, Switzerland. 669–716.
5. Song, P.-S., P. Koka, B. B. Prezelin, and F. T. Haxo. 1976. Molecular topology of photosynthetic light-harvesting pigment complex, peridinin-chlorophyll-a-protein, from marine dinoflagellates. *Biochemistry.* 15:4422–4427.
6. Koka, P., and P.-S. Song. 1977. The chromophore topography and binding environment of peridinin-chlorophyll a-protein complexes from marine dinoflagellate algae. *Biochim. Biophys. Acta.* 495: 220–231.
7. Mimuro, M., U. Nagashima, S. Nagaoka, Y. Nishimura, S. Takaichi, T. Katoh, and I. Yamazaki. 1992. Quantitative-analysis of the solvent effect on the relaxation processes of carotenoids showing dual emissive characteristics. *Chem. Phys. Lett.* 191:219–224.
8. Mimuro, M., Y. Nishimura, S. Takaichi, Y. Yamano, M. Ito, S. Nagaoka, I. Yamazaki, T. Katoh, and U. Nagashima. 1993. The effect of molecular-structure on the relaxation processes of carotenoids containing a carbonyl group. *Chem. Phys. Lett.* 213:576–580.
9. Bautista, J. A., R. G. Hiller, F. P. Sharples, D. Gosztola, M. Wasielewski, and H. A. Frank. 1999. Singlet and triplet energy transfer in the peridinin-chlorophyll a protein from Amphidinium carterae. *J. Phys. Chem. A.* 103:2267–2273.
10. Krueger, B. P., S. S. Lampoura, I. H. M. van Stokkum, E. Papagiannakis, J. M. Salverda, C. C. Gradinaru, D. Rutkauskas, R. G. Hiller, and R. van Grondelle. 2001. Energy transfer in the peridinin chlorophyll-a protein of Amphidinium carterae studied by polarized transient absorption and target analysis. *Biophys. J.* 80:2843–2855.
11. Kleima, F. J., M. Wendling, E. Hofmann, E. J. G. Peterman, R. van Grondelle, and H. van Amerongen. 2000. Peridinin chlorophyll a protein: relating structure and steady-state spectroscopy. *Biochemistry.* 39: 5184–5195.
12. Damjanovic, A., T. Ritz, and K. Schulten. 1999. Energy transfer between carotenoids and bacteriochlorophylls in a light harvesting protein. *Physical Review E.* 59:3293–3311.
13. Damjanovic, A., T. Ritz, and K. Schulten. 2000. Excitation transfer in the peridinin-chlorophyll-protein of *Amphidinium carterae*. *Biophys. J.* 79:1695–1705.
14. Nagae, H., T. Kakitani, T. Katoh, and M. Mimuro. 1993. Calculation of the excitation transfer-matrix elements between the S(2) or S(1) state of carotenoid and the S(2) or S(1). State of bacteriochlorophyll. *J. Chem. Phys.* 98:8012–8023.
15. Krueger, B. P., G. D. Scholes, R. Jimenez, and G. R. Fleming. 1998. Electronic excitation transfer from carotenoid to bacteriochlorophyll in the purple bacterium *Rhodopseudomonas acidophila*. *J. Phys. Chem. B.* 102:2284–2292.
16. Krueger, B. P., G. D. Scholes, and G. R. Fleming. 1998. Calculation of couplings and energy-transfer pathways between the pigments of LH2 by the *ab initio* transition density cube method. *J. Phys. Chem. B.* 102: 5378–5386.
17. Frank, H. A., and R. J. Cogdell. 1996. Carotenoids in photosynthesis. *Photochem. Photobiol.* 63:257–264.
18. Cogdell, R. J., T. D. Howard, R. Bittl, E. Schlodder, I. Geisenheimer, and W. Lubitz. 2000. How carotenoids protect bacterial photosynthesis. *Philos. Trans. R. Soc. Lond. B Biol. Sci.* 355:1345–1349.
19. Bensasson, R., E. J. Land, and B. Maudinas. 1976. Triplet-states of carotenoids from photosynthetic bacteria studied by nanosecond ultraviolet and electron pulse irradiation. *Photochem. Photobiol.* 18:189–193.
20. Mathis, P., and J. Kleo. 1973. Triplet-state of beta-carotene and of analog polyenes of different length. *Photochem. Photobiol.* 18:343–346.
21. Siefermann-Harms, D. 1987. The light-harvesting and protective functions of carotenoids in photosynthetic membranes. *Physiol. Plant.* 69:561–568.
22. Cogdell, R. J., and H. A. Frank. 1987. How carotenoids function in photosynthetic bacteria. *Biochim. Biophys. Acta.* 895:63–79.
23. Tandori, J., E. Hideg, L. Nagy, P. Maroti, and I. Vass. 2001. Photoinhibition of carotenoidless reaction centers from Rhodobacter sphaeroides by visible light. Effects on protein structure and electron transport. *Photosynth. Res.* 70:175–184.
24. Zigmantas, D., R. G. Hiller, V. Sundström, and T. Polivka. 2002. Carotenoid to chlorophyll energy transfer in the peridinin-chlorophyll-*a*-protein complex involves an intramolecular charge transfer state. *Proc. Natl. Acad. Sci. USA.* 99:16760–16765.
25. Dexter, D. L. 1953. A theory of sensitized luminescence in solids. *J. Chem. Phys.* 21:834–850.
26. Carbonera, D., G. Giacometti, U. Segre, A. Angerhofer, and U. Gross. 1999. Model for triplet-triplet energy transfer in natural clusters of peridinin molecules contained in dinoflagellate's outer antenna proteins. *J. Phys. Chem. B.* 103:6357–6362.
27. Carbonera, D., G. Giacometti, and U. Segre. 1996. Carotenoid interactions in peridinin chlorophyll a proteins from dinoflagellates: evidence for optical excitons and triplet migration. *J. Chem. Soc. Faraday Transactions.* 92:989–993.
28. Peterman, E. J. G., F. M. Dukker, R. van Grondelle, and H. van Amerongen. 1995. Chlorophyll a and carotenoid triplet states in light-harvesting complex II of higher plants. *Biophys. J.* 69:2670–2678.
29. Van der Vos, R., D. Carbonera, and A. J. Hoff. 1991. Microwave and optical spectroscopy of carotenoid triplets in light-harvesting complex LHC II of spinach by absorbance-detected magnetic resonance. *Appl. Magn. Res.* 2:179–202.
30. Angerhofer, A., F. Bornhauser, A. Gall, and R. J. Cogdell. 1995. Optical and optically detected magnetic-resonance investigation on purple photosynthetic bacterial antenna complexes. *Chem. Phys.* 194: 259–274.
31. Holzwarth, A. R. 1996. Data analysis of time-resolved measurements. *In* Biophysical Techniques in Photosynthesis. J. Amesz and A. J. Hoff, editors. Kluwer, Dordrecht, The Netherlands. 75–92.
32. van Stokkum, I. H. M., D. S. Larsen, and R. van Grondelle. 2004. Global and target analysis of time-resolved spectra. *Biochim. Biophys. Acta.* 1657:82–104.
33. Gurzadyan, G. G., and S. Steenken. 2002. Photoionization of beta-carotene via electron transfer from excited states to chlorinated hydrocarbon solvents. A picosecond transient absorption study. *Phys. Chem. Chem. Phys.* 4:2983–2988.
34. Hashimoto, H., Y. Koyama, Y. Hirata, and N. Mataga. 1991. S1 and T1 species of β-carotene generated by direct photo-excitation from the all-*trans*, 9-*cis*, 13-*cis* and 15-*cis* isomers as revealed by picosecond transient absorption and transient Raman spectroscopies. *J. Phys. Chem.* 95:3072–3076.
35. Noguchi, T., H. Hayashi, M. Tasumi, and G. H. Atkinson. 1990. Frequencies of the Franck-Condon active a_g C=C stretching mode in the 2 $1A_g^-$ excited state of carotenoids. *Chem. Phys. Lett.* 175:163–169.
36. Nagae, H., M. Kuki, J.-P. Zhang, T. Sashima, Y. Mukai, and Y. Koyama. 2000. Vibronic coupling through the in-phase, C=C stretching mode plays a major role in the 2Ag- to 1Ag-internal conversion of all-*trans* carotene. *J. Phys. Chem. A.* 104:4155–4166.
37. Bernhard, K., and M. Grosjean. 1995. Infrared spectroscopy. *In* Carotenoids. G. Britton, S. Liaaen-Jensen, and H. Pfander, editors. Birkhäuser. Basel, Switzerland.
38. Breton, J., E. Nabedryk, and W. Leibl. 1999. FTIR study of the primary electron donor of photosystem I (P700) revealing delocalization of the charge in P700(+) and localization of the triplet character in (3)P700. *Biochemistry.* 38:11585–11592.
39. Breton, J. 2001. Fourier transform infrared spectroscopy of primary electron donors in type I photosynthetic reaction centers. *Biochim. Biophys. Acta.* 1507:180–193.
40. Noguchi, T. 2002. Dual role of triplet localization on the accessory chlorophyll in the photosystem II reaction center: photoprotection and photodamage of the D1 protein. *Plant Cell Physiol.* 43:1112–1116.
41. Mantele, W. G., A. M. Wollenweber, E. Nabedryk, and J. Breton. 1988. Infrared spectroelectrochemistry of bacteriochlorophylls and bacteriopheophytins: implications for the binding of the pigments in

the reaction center from photosynthetic bacteria. *Proc. Natl. Acad. Sci. USA.* 85:8468–8472.

42. Okubo, T., and T. Noguchi. 2007. Selective detection of the structural changes upon photoreactions of several redox cofactors in photosystem II by means of light-induced ATR-FTIR difference spectroscopy. *Spectrochim. Acta A Mol. Biomol. Spectrosc.* 66:863–868.
43. Hartwich, G., C. Geskes, H. Scheer, J. Heinze, and W. Mantele. 1995. Fourier-transform infrared-spectroscopy of electrogenerated anions and cations of metal-substituted bacteriochlorophyll-alpha. *J. Am. Chem. Soc.* 117:7784–7790.
44. Kristallovich, E. L., I. D. Shamyanov, M. R. Yagudaev, and V. M. Malikov. 1987. Frequencies and integral intensities of lactone and ester carbonyls of natural guaianolides. *Him. Prir. Soedin.* 6:805–811.
45. Peterman, E. J. G., C. Gradinaru, F. Calkoen, J. C. Borst, R. van Grondelle, and H. van Amerongen. 1997. Xanthophylls in light-harvesting complex II of higher plants: light harvesting and triplet quenching. *Biochemistry.* 36:12208–12215.
46. Akimoto, S., S. Takaichi, T. Ogata, Y. Nishimura, I. Yamazaki, and M. Mimuro. 1996. Excitation energy transfer in carotenoid-chlorophyll protein complexes probed by femtosecond fluorescence decays. *Chem. Phys. Lett.* 260:147–152.
47. Rondonuwu, F. S., T. Taguchi, R. Fujii, K. Yokoyama, Y. Koyama, and Y. Watanabe. 2004. The energies and kinetics of triplet carotenoids in the LH2 antenna complexes as determined by phosphorescence spectroscopy. *Chem. Phys. Lett.* 384:364–371.
48. Takiff, L., and S. G. Boxer. 1988. Phosphorescence spectra of bacteriochlorophylls. *J. Am. Chem. Soc.* 110:4425–4426.
49. You, Z. Q., C. P. Hsu, and G. R. Fleming. 2006. Triplet-triplet energy-transfer coupling: theory and calculation. *J. Chem. Phys.* 124:044506.
50. Kodis, G., C. Herrero, R. Palacios, E. Marino-Ochoa, S. Gould, L. de la Garza, R. van Grondelle, D. Gust, T. A. Moore, A. L. Moore, and J. T. M. Kennis. 2004. Light harvesting and photoprotective functions of carotenoids in compact artificial photosynthetic antenna designs. *J. Phys. Chem. B.* 108:414–425.
51. Berera, R., C. Herrero, L. H. M. van Stokkum, M. Vengris, G. Kodis, R. E. Palacios, H. van Amerongen, R. van Grondelle, D. Gust, T. A. Moore, A. L. Moore, and J. T. M. Kennis. 2006. A simple artificial light-harvesting dyad as a model for excess energy dissipation in oxygenic photosynthesis. *Proc. Natl. Acad. Sci. USA.* 103:5343–5348.
52. Premvardhan, L., E. Papagiannakis, R. G. Hiller, and R. van Grondelle. 2005. The charge-transfer character of the S0→S2 transition in the carotenoid peridinin is revealed by Stark spectroscopy. *J. Phys. Chem. B Condens Matter Mater Surf Interfaces Biophys.* 109:15589–15597.
53. Frese, R. 2003. Symmetry in photosynthesis. PhD thesis. Vrije Unversiteit, Amsterdam.
54. Salverda, J. M. 2003. Interacting pigments in light-harvesting complexes studied with nonlinear spectroscopy. PhD thesis. Vrije Universiteit, Amsterdam. Chapter 6.
55. Carbonera, D., G. Giacometti, U. Segre, E. Hofmann, and R. G. Hiller. 1999. Structure-based calculations of the optical spectra of the light-harvesting peridinin-chlorophyll-protein complexes from Amphidinium carterae and Heterocapsa pygmaea. *J. Phys. Chem. B.* 103: 6349–6356.
56. Papagiannakis, E., J. T. M. Kennis, I. H. M. van Stokkum, R. J. Cogdell, and R. van Grondelle. 2002. An alternative carotenoid-to-bacteriochlorophyll energy transfer pathway in photosynthetic light harvesting. *Proc. Natl. Acad. Sci. USA.* 99:6017–6022.
57. Gradinaru, C. C., J. T. M. Kennis, E. Papagiannakis, I. H. M. van Stokkum, R. J. Cogdell, G. R. Fleming, R. A. Niederman, and R. van Grondelle. 2001. An unusual pathway of excitation energy deactivation in carotenoids: singlet-to-triplet conversion on an ultrafast timescale in a photosynthetic antenna. *Proc. Natl. Acad. Sci. USA.* 98:2364–2369.
58. Papagiannakis, E., S. K. Das, A. Gall, I. H. M. van Stokkum, B. Robert, R. van Grondelle, H. A. Frank, and J. T. M. Kennis. 2003. Light harvesting by carotenoids incorporated into the B850 light-harvesting complex from Rhodobacter sphaeroides R-26.1: excited-state relaxation, ultrafast triplet formation, and energy transfer to bacteriochlorophyll. *J. Phys. Chem. B.* 107:5642–5649.
59. Papagiannakis, E., M. Vengris, D. S. Larsen, I. H. M. van Stokkum, R. G. Hiller, and R. van Grondelle. 2006. Use of ultrafast dispersed pump-dump-probe and pump-repump-probe spectroscopies to explore the light-induced dynamics of peridinin in solution. *J. Phys. Chem. B.* 110:512–521.
60. Billsten, H. H., J. X. Pan, S. Sinha, T. Pascher, V. Sundstrom, and T. Polivka. 2005. Excited-state processes in the carotenoid zeaxanthin after excess energy excitation. *J. Phys. Chem. A.* 109:6852–6859.
61. Bittl, R., E. Schlodder, I. Geisenheimer, W. Lubitz, and R. J. Cogdell. 2001. Transient EPR and absorption studies of carotenoid triplet formation in purple bacterial antenna complexes. *J. Phys. Chem. B.* 105:5525–5535.
62. Schödel, R., K. D. Irrgang, J. Voigt, and G. Renger. 1998. Rate of carotenoid triplet formation in solubilized light-harvesting complex II (LHCII) from spinach. *Biophys. J.* 75:3143–3153.